

Study of beauty hadron decays into Pairs of charm hadrons

LHCb Collaboration

DOI:

[10.1103/PhysRevLett.112.202001](https://doi.org/10.1103/PhysRevLett.112.202001)

License:

Creative Commons: Attribution (CC BY)

Document Version

Publisher's PDF, also known as Version of record

Citation for published version (Harvard):

LHCb Collaboration 2014, 'Study of beauty hadron decays into Pairs of charm hadrons', *Physical Review Letters*, vol. 112, no. 20, 202001. <https://doi.org/10.1103/PhysRevLett.112.202001>

[Link to publication on Research at Birmingham portal](#)

General rights

Unless a licence is specified above, all rights (including copyright and moral rights) in this document are retained by the authors and/or the copyright holders. The express permission of the copyright holder must be obtained for any use of this material other than for purposes permitted by law.

- Users may freely distribute the URL that is used to identify this publication.
- Users may download and/or print one copy of the publication from the University of Birmingham research portal for the purpose of private study or non-commercial research.
- User may use extracts from the document in line with the concept of 'fair dealing' under the Copyright, Designs and Patents Act 1988 (?)
- Users may not further distribute the material nor use it for the purposes of commercial gain.

Where a licence is displayed above, please note the terms and conditions of the licence govern your use of this document.

When citing, please reference the published version.

Take down policy

While the University of Birmingham exercises care and attention in making items available there are rare occasions when an item has been uploaded in error or has been deemed to be commercially or otherwise sensitive.

If you believe that this is the case for this document, please contact UBIRA@lists.bham.ac.uk providing details and we will remove access to the work immediately and investigate.

Study of Beauty Hadron Decays into Pairs of Charm Hadrons

R. Aaij *et al.**

(LHCb Collaboration)

(Received 17 March 2014; published 21 May 2014)

First observations of the decays $\Lambda_b^0 \rightarrow \Lambda_c^+ D_{(s)}^-$ are reported using data corresponding to an integrated luminosity of 3 fb^{-1} collected at 7 and 8 TeV center-of-mass energies in proton-proton collisions with the LHCb detector. In addition, the most precise measurement of the branching fraction $\mathcal{B}(B_s^0 \rightarrow D^+ D_s^-)$ is made and a search is performed for the decays $B_{(s)}^0 \rightarrow \Lambda_c^+ \Lambda_c^-$. The results obtained are

$$\begin{aligned} \mathcal{B}(\Lambda_b^0 \rightarrow \Lambda_c^+ D^-) / \mathcal{B}(\Lambda_b^0 \rightarrow \Lambda_c^+ D_s^-) &= 0.042 \pm 0.003(\text{stat}) \pm 0.003(\text{syst}), \\ \frac{\mathcal{B}(\Lambda_b^0 \rightarrow \Lambda_c^+ D_s^-)}{\mathcal{B}(\bar{B}^0 \rightarrow D^+ D_s^-)} / \frac{\mathcal{B}(\Lambda_b^0 \rightarrow \Lambda_c^+ \pi^-)}{\mathcal{B}(\bar{B}^0 \rightarrow D^+ \pi^-)} &= 0.96 \pm 0.02(\text{stat}) \pm 0.06(\text{syst}), \\ \mathcal{B}(B_s^0 \rightarrow D^+ D_s^-) / \mathcal{B}(\bar{B}^0 \rightarrow D^+ D_s^-) &= 0.038 \pm 0.004(\text{stat}) \pm 0.003(\text{syst}), \\ \mathcal{B}(\bar{B}^0 \rightarrow \Lambda_c^+ \Lambda_c^-) / \mathcal{B}(\bar{B}^0 \rightarrow D^+ D_s^-) &< 0.0022[95\% \text{ C.L.}], \\ \mathcal{B}(B_s^0 \rightarrow \Lambda_c^+ \Lambda_c^-) / \mathcal{B}(B_s^0 \rightarrow D^+ D_s^-) &< 0.30[95\% \text{ C.L.}]. \end{aligned}$$

Measurement of the mass of the Λ_b^0 baryon relative to the \bar{B}^0 meson gives $M(\Lambda_b^0) - M(\bar{B}^0) = 339.72 \pm 0.24(\text{stat}) \pm 0.18(\text{syst}) \text{ MeV}/c^2$. This result provides the most precise measurement of the mass of the Λ_b^0 baryon to date.

DOI: 10.1103/PhysRevLett.112.202001

PACS numbers: 14.20.Mr, 13.30.—a

Hadrons are systems of quarks bound by the strong interaction, described at the fundamental level by quantum chromodynamics (QCD). Low-energy phenomena, such as the binding of quarks and gluons within hadrons, lie in the nonperturbative regime of QCD and are difficult to calculate. Much progress has been made in recent years in the study of beauty mesons [1]; however, many aspects of beauty baryons are still largely unknown. Many decays of beauty mesons into pairs of charm hadrons have branching fractions at the percent level [2]. Decays of beauty baryons into pairs of charm hadrons are expected to be of comparable size, yet none have been observed to date. If such decays do have sizable branching fractions, they could be used to study beauty-baryon properties. For example, a comparison of beauty meson and baryon branching fractions can be used to test factorization in these decays [3].

Many models and techniques have been developed that attempt to reproduce the spectrum of the measured hadron masses, such as constituent-quark models or lattice QCD calculations [4]. Precise measurements of ground-state beauty-baryon masses are required to permit precision tests of a variety of QCD models [5–11]. The Λ_b^0 baryon mass is particularly interesting in this context, since several

ground-state beauty-baryon masses are measured relative to that of the Λ_b^0 [12].

This Letter reports the first observation of the decays $\Lambda_b^0 \rightarrow \Lambda_c^+ D_s^-$ and $\Lambda_b^0 \rightarrow \Lambda_c^+ D^-$. The decay $\Lambda_b^0 \rightarrow \Lambda_c^+ D_s^-$ is used to make the most precise measurement to date of the mass of the Λ_b^0 baryon. Improved measurements of the branching fraction $\mathcal{B}(B_s^0 \rightarrow D^+ D_s^-)$ and stringent upper limits on $\mathcal{B}(B_{(s)}^0 \rightarrow \Lambda_c^+ \Lambda_c^-)$ are also reported. Charge conjugated decay modes are implied throughout this Letter. The data used correspond to an integrated luminosity of 1 and 2 fb^{-1} collected at 7 and 8 TeV center-of-mass energies in pp collisions, respectively, with the LHCb detector.

The LHCb detector is a single-arm forward spectrometer covering the pseudorapidity range $2 < \eta < 5$, described in detail in Refs. [13–18]. Samples of simulated events are used to determine selection efficiencies, to model candidate distributions, and to investigate possible background contributions. In the simulation, pp collisions are generated using PYTHIA [19] with a specific LHCb configuration [20]. Decays of hadronic particles are described by EVTGEN [21], in which final-state radiation is generated using PHOTOS [22]. The interaction of the generated particles with the detector and its response are implemented using the GEANT4 toolkit [23] as described in Ref. [24].

In this analysis, signal beauty-hadron candidates are formed by combining charm-hadron candidate pairs reconstructed in the following decay modes: $D^+ \rightarrow K^- \pi^+ \pi^+$, $D_s^+ \rightarrow K^- K^+ \pi^+$, and $\Lambda_c^+ \rightarrow p K^- \pi^+$. The measured invariant mass of each charm-hadron candidate, the resolution on

* Full author list given at the end of the article.

Published by the American Physical Society under the terms of the Creative Commons Attribution 3.0 License. Further distribution of this work must maintain attribution to the author(s) and the published articles title, journal citation, and DOI.

which is about $6 - 8 \text{ MeV}/c^2$, is required to be within $25 \text{ MeV}/c^2$ of the nominal value [2]. To improve the resolution of the beauty-hadron mass, the decay chain is fit imposing kinematic and vertex constraints [25]; this includes constraining the charm-hadron masses to their nominal values. To suppress contributions from noncharm decays, the reconstructed charm-hadron decay vertex is required to be downstream of, and significantly displaced from, the reconstructed beauty-hadron decay vertex.

A boosted decision tree (BDT) [26] is used to select each type of charm-hadron candidate. These BDTs use five variables for the charm hadron and 23 for each of its decay products. The variables include kinematic quantities, track and vertex qualities, and particle identification (PID) information. The signal samples used to train the BDTs are obtained from large data sets of $\bar{B}^0 \rightarrow D^+ \pi^-$, $\bar{B}_s^0 \rightarrow D_s^+ \pi^-$, and $\Lambda_b^0 \rightarrow \Lambda_c^+ \pi^-$ decays that are background subtracted using weights [27] obtained from fits to the beauty-hadron invariant mass distributions. The background data samples are taken from the charm-hadron and high-mass beauty-hadron sidebands in the same data sets. To obtain the BDT efficiency in a given signal decay mode, the kinematical properties and correlations between the two charm hadrons are taken from simulation. The BDT response distributions are obtained from independent data samples of the decays used in the BDT training, weighted to match the kinematics of the signal.

Because of the kinematic similarity of the decays $D^+ \rightarrow K^- \pi^+ \pi^+$, $D_s^+ \rightarrow K^- K^+ \pi^+$, and $\Lambda_c^+ \rightarrow p K^- \pi^+$, cross feed may occur among beauty-hadron decays into pairs of charm hadrons. For example, cross feed between D^+ and D_s^+ mesons occurs when a $K^- h^+ \pi^+$ candidate is reconstructed in the D^+ mass region under the $h^+ = \pi^+$ hypothesis and in the D_s^+ mass region under the $h^+ = K^+$ hypothesis. In such situations, an arbitration is performed: if the ambiguous track (h^+) can be associated to an oppositely charged track to form a $\phi(1020) \rightarrow K^+ K^-$ candidate, the kaon hypothesis is taken, resulting in a D_s^+ assignment to the charm-hadron candidate; otherwise, stringent PID requirements are applied to h^+ to choose which hypothesis to take. The efficiency of these arbitrations, which is found to be about 90% per charm hadron, is obtained using simulated signal decays to model the kinematical properties and $D^{*+} \rightarrow D^0 \pi^+$ calibration data for the PID efficiencies. The misidentification probability is roughly 1% per charm hadron.

Signal yields are determined by performing unbinned extended likelihood fits to the beauty-hadron invariant-mass spectra observed in the data. The signal distributions are modeled using a so-called Apollonios function, which is the exponential of a hyperbola combined with a power-law low-mass tail [28]. The peak position and resolution parameters are allowed to vary while fitting the data, while the low-mass tail parameters are taken from simulation and fixed in the fits.

Four categories of background contributions are considered: partially reconstructed decays of beauty hadrons where at least one final-state particle is not reconstructed; decays into a single charm hadron and three light hadrons; reflections, defined as cases where the cross-feed arbitration fails to remove a misidentified particle; and combinatorial background. The only partially reconstructed decays that contribute in the mass region studied are those where a single pion or photon is not reconstructed; thus, only final states comprised of D_c^{*+} or Σ_c^+ and another charm hadron are considered (e.g., $\Lambda_b^{(s)+} \rightarrow \Lambda_c^+ D_s^{*-}$). These background contributions are modeled using kernel probability density functions (PDFs) [29] obtained from simulation; their yields are free to vary in the fits. Single-charm backgrounds are studied using data that are reconstructed outside of a given charm-hadron mass region. These backgrounds are found to be $\mathcal{O}(1\%)$ of the size of the signal yield for signal decays containing a D_s^- (e.g., $\bar{B}^0 \rightarrow D^+ K^- K^+ \pi^-$) and are negligible otherwise. The only non-negligible reflection is found to be $\Lambda_b^0 \rightarrow \Lambda_c^+ D_s^-$ decays misidentified as $\Lambda_c^+ D^-$ candidates. The invariant-mass distribution for this reflection is obtained from simulation, while the normalization is fixed using simulation and the aforementioned PID calibration sample to determine the fraction of $\Lambda_b^0 \rightarrow \Lambda_c^+ D_s^-$ decays that are not removed by the cross-feed criteria. Reflections of $\bar{B}^0 \rightarrow D^+ D_s^-$ decays misidentified as final states containing Λ_c^+ particles do not have a peaking structure in the beauty-hadron invariant mass and, therefore, are absorbed into the combinatorial backgrounds, which are modeled using exponential distributions.

Figure 1 shows the invariant mass spectra for the $\Lambda_b^0 \rightarrow \Lambda_c^+ D_s^-$ and $\Lambda_b^0 \rightarrow \Lambda_c^+ D^-$ candidates. The signal yields obtained are 4633 ± 69 and 262 ± 19 for $\Lambda_b^0 \rightarrow \Lambda_c^+ D_s^-$ and $\Lambda_b^0 \rightarrow \Lambda_c^+ D^-$, respectively. This is the first observation of each of these decays. The ratio of branching fractions determined using the nominal D_s^- [2] and D^- [30] meson branching fractions and the ratio of efficiencies is

$$\frac{\mathcal{B}(\Lambda_b^0 \rightarrow \Lambda_c^+ D^-)}{\mathcal{B}(\Lambda_b^0 \rightarrow \Lambda_c^+ D_s^-)} = 0.042 \pm 0.003(\text{stat}) \pm 0.003(\text{syst}).$$

The similarity of the final states and the shared parent particle result in many cancellations of uncertainties in the determination of the ratio of branching fractions. The remaining uncertainties include roughly equivalent contributions from determining the efficiency-corrected yields and from the ratio of charm-hadron branching fractions (see Table I). The dominant contribution to the uncertainty of the fit PDF is due to the low-mass background contributions, which are varied in size and shape to determine the effect on the signal yield. The uncertainty due to signal model is found to be negligible. The efficiencies of the cross feed and BDT criteria are determined in a data-driven manner that produces small uncertainties. The observed ratio is approximately the ratio of the relevant quark-mixing

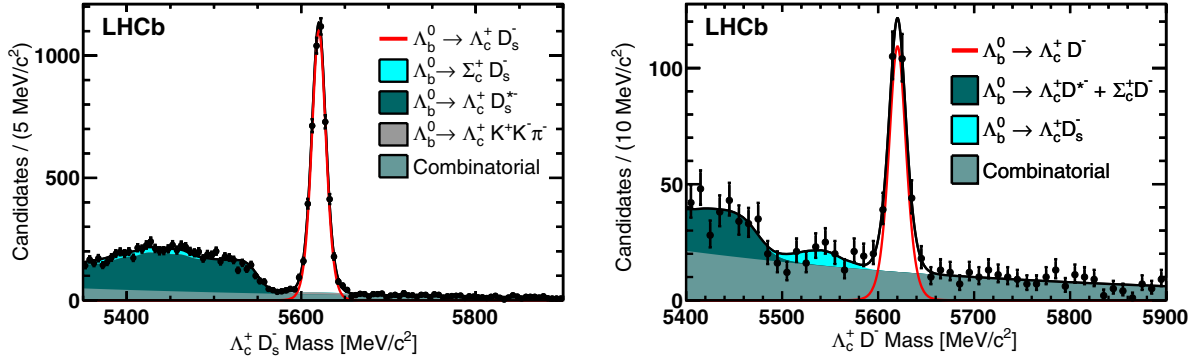


FIG. 1 (color online). Invariant mass distributions for (left) $\Lambda_b^0 \rightarrow \Lambda_c^+ D_s^-$ and (right) $\Lambda_b^0 \rightarrow \Lambda_c^+ D^-$ candidates with the fits described in the text overlaid.

factors and meson decay constants, $|V_{cd}/V_{cs}|^2 \times (f_D/f_{D_s})^2 \approx 0.034$, as expected assuming nonfactorizable effects are small.

The branching fraction of the decay $\Lambda_b^0 \rightarrow \Lambda_c^+ D_s^-$ is determined relative to that of the $\bar{B}^0 \rightarrow D^+ D_s^-$ decay. Using $D^+ D_s^-$ BDT criteria optimized to maximize the expected \bar{B}^0 significance, $19\,395 \pm 145$ $\bar{B}^0 \rightarrow D^+ D_s^-$ decays are observed (see Fig. 2). The measurement of $\mathcal{B}(\Lambda_b^0 \rightarrow \Lambda_c^+ D_s^-)/\mathcal{B}(\bar{B}^0 \rightarrow D^+ D_s^-)$ is complicated by the fact that the ratio of the Λ_b^0 and \bar{B}^0 production cross sections, $\sigma(\Lambda_b^0)/\sigma(\bar{B}^0)$, depends on the p_T of the beauty hadrons [32]. Figure 3 shows the ratio of efficiency-corrected yields, $N(\Lambda_b^0 \rightarrow \Lambda_c^+ D_s^-)/N(\bar{B}^0 \rightarrow D^+ D_s^-)$, as a function of beauty-hadron p_T . The ratio of branching-fraction ratios is obtained using a fit with the shape of the p_T dependence measured in $\mathcal{B}(\Lambda_b^0 \rightarrow \Lambda_c^+ \pi^-)/\mathcal{B}(\bar{B}^0 \rightarrow D^+ \pi^-)$ [33] and found to be

$$\frac{\left[\frac{\mathcal{B}(\Lambda_b^0 \rightarrow \Lambda_c^+ D_s^-)}{\mathcal{B}(\bar{B}^0 \rightarrow D^+ D_s^-)}\right]}{\left[\frac{\mathcal{B}(\Lambda_b^0 \rightarrow \Lambda_c^+ \pi^-)}{\mathcal{B}(\bar{B}^0 \rightarrow D^+ \pi^-)}\right]} = 0.96 \pm 0.02(\text{stat}) \pm 0.06(\text{syst}).$$

This result does not depend on the absolute ratio of production cross sections or on any charm-hadron branching fractions. The systematic uncertainties on this result are listed in Table I. The uncertainty in the fit model is due largely to the sizable single-charm background contributions to these

modes and to contributions from the fits described in Ref. [33]. The $\mathcal{B}(\Lambda_b^0 \rightarrow \Lambda_c^+ \pi^-)/\mathcal{B}(\bar{B}^0 \rightarrow D^+ \pi^-)$ result was obtained only using data collected at $\sqrt{s} = 7$ TeV. The ratio $N(\Lambda_b^0 \rightarrow \Lambda_c^+ D_s^-)/N(\bar{B}^0 \rightarrow D^+ D_s^-)$ is observed to be consistent in data collected at $\sqrt{s} = 7$ and 8 TeV. The statistical uncertainty on this comparison is assigned as the systematic uncertainty on the energy dependence of the Λ_b^0 and \bar{B}^0 production fractions. The ratio of branching ratios is consistent with unity, as expected assuming small nonfactorizable effects.

The kinematic similarity of the decay modes $\Lambda_b^0 \rightarrow \Lambda_c^+ D_s^-$ and $\bar{B}^0 \rightarrow D^+ D_s^-$ permits a precision measurement of the mass difference of the Λ_b^0 and \bar{B}^0 hadrons. The relatively small value of $[M(\Lambda_b^0) - M(\Lambda_c^+) - M(D_s^-)] - [M(\bar{B}^0) - M(D^+) - M(D_s^-)]$ means that the uncertainty due to momentum scale, the dominant uncertainty in absolute-mass measurements, mostly cancels; however, it is still important to determine accurately the momenta of the final-state particles. The momentum-scale calibration of the spectrometer, which accounts for imperfect knowledge of the magnetic field and alignment, is discussed in detail in Refs. [12,34]. The uncertainty on the calibrated momentum scale is estimated to be 0.03% by comparing various particle masses measured at LHCb to their nominal values [34].

The kinematic and vertex constraints used in the fits described previously reduce the statistical uncertainty on $M(\Lambda_b^0) - M(\bar{B}^0)$ by improving the resolution. These

TABLE I. Relative systematic uncertainties on branching fraction measurements (%). The production ratio $\sigma(B_s^0)/\sigma(\bar{B}^0)$ is taken from Ref. [31]. The numbers in parentheses in the last column are for the B_s^0 decay mode.

Source	$\mathcal{B}(\Lambda_b^0 \rightarrow \Lambda_c^+ D^-)/\mathcal{B}(\Lambda_b^0 \rightarrow \Lambda_c^+ D_s^-)$	$([\mathcal{B}(\Lambda_b^0 \rightarrow \Lambda_c^+ D_s^-)/\mathcal{B}(\bar{B}^0 \rightarrow D^+ D_s^-)]/[\mathcal{B}(\Lambda_b^0 \rightarrow \Lambda_c^+ \pi^-)/\mathcal{B}(\bar{B}^0 \rightarrow D^+ \pi^-)])$	$\mathcal{B}(B_s^0 \rightarrow D^+ D_s^-)/\mathcal{B}(\bar{B}^0 \rightarrow D^+ D_s^-)$	$\mathcal{B}(B_{(s)}^0 \rightarrow \Lambda_c^+ \Lambda_c^-)/\mathcal{B}(B_{(s)}^0 \rightarrow D^+ D_s^-)$
Efficiency	3.5	5.2	1.0	3.9 (5.0)
Fit model	3.0	2.6	3.0	...
$\mathcal{B}(D_{(s)}^+, \Lambda_c^+)$	5.2	8.8
$\sigma(B_s^0)/\sigma(\bar{B}^0)$	5.8	...
$\sigma(\Lambda_b^0)/\sigma(\bar{B}^0)$...	2.0
Total	6.9	6.1	6.6	9.6 (10.1)

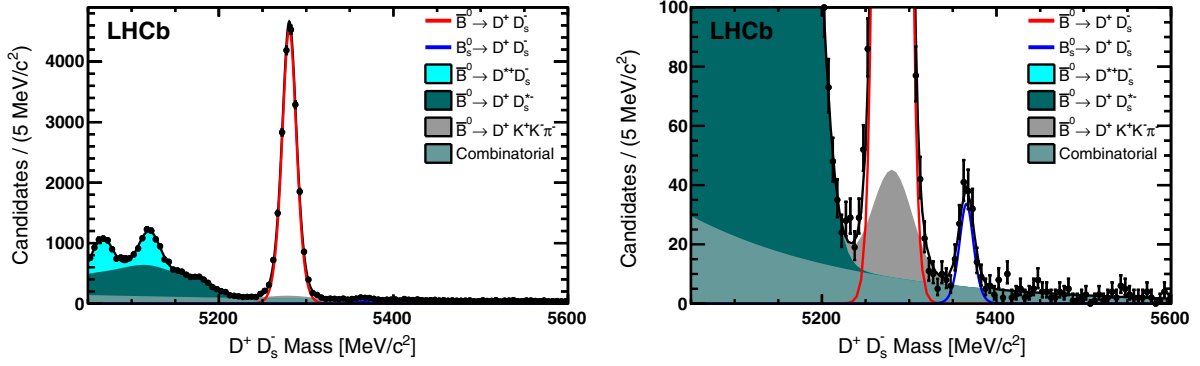


FIG. 2 (color online). Invariant mass distributions for $D^+ D_s^-$ candidates selected using BDT criteria optimized for the (left) $\bar{B}^0 \rightarrow D^+ D_s^-$ and (right) $B_s^0 \rightarrow D^+ D_s^-$ decay modes with the fits described in the text overlaid.

constraints also increase the systematic uncertainty by introducing a dependence on the precision of the nominal charm-hadron masses. These constraints are not imposed in the mass measurement, as it is found that this approach produces a smaller total uncertainty. The mass difference obtained is

$$M(\Lambda_b^0) - M(\bar{B}^0) = 339.72 \pm 0.24(\text{stat}) \\ \pm 0.18(\text{syst}) \text{ MeV}/c^2.$$

The dominant systematic uncertainty (see Table II) arises due to a correlation between the reconstructed beauty-hadron mass and reconstructed charm-hadron flight distance. The large difference in the Λ_c^+ and D^+ hadron lifetimes [2] could lead to only a partial cancellation of the biases induced by the charm-lifetime selection criteria. This effect is studied in simulation and a $0.16 \text{ MeV}/c^2$ uncertainty is assigned. The 0.03% uncertainty in the momentum scale results in an uncertainty on the mass difference of $0.08 \text{ MeV}/c^2$. Many variations in the fit model are considered, and none produce a significant shift in the mass

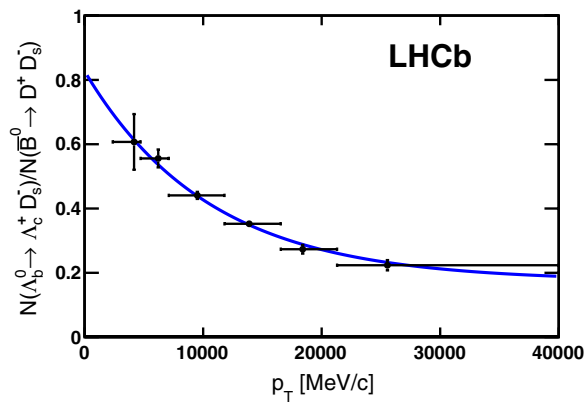


FIG. 3 (color online). Efficiency-corrected ratio of the yields of $\Lambda_b^0 \rightarrow \Lambda_c^+ D_s^-$ and $\bar{B}^0 \rightarrow D^+ D_s^-$ vs p_T . The points are located at the mean p_T value of the Λ_b^0 in each bin. The curve shows the data fit with the shape of the p_T dependence measured in Ref. [33].

difference. The systematic uncertainty in the mass difference due to the uncertainty in the amount of detector material in which charged particles lose energy is negligible [34]. Furthermore, the uncertainty on $M(\Lambda_b^0) - M(\bar{B}^0)$ due to differences in beauty-hadron production kinematics, as seen in Fig. 3, is also found to be negligible.

Using the nominal value for $M(\bar{B}^0)$ [2] gives $M(\Lambda_b^0) = 5619.30 \pm 0.34 \text{ MeV}/c^2$, where the uncertainty includes both statistical and systematic contributions. This is the most precise result to date. The total uncertainty is dominated by statistics and charm-hadron lifetime effects; thus, this result can be treated as being uncorrelated with the previous LHCb result obtained using the $\Lambda_b^0 \rightarrow J/\psi \Lambda^0$ decay [35]. A weighted average of the LHCb results gives $M(\Lambda_b^0) = 5619.36 \pm 0.26 \text{ MeV}/c^2$. This value may then be used to improve the precision of the Ξ_b^- and Ω_b^- baryon masses using their mass differences with respect to the Λ_b^0 baryon, as reported in Ref. [35].

Using BDT criteria optimized for maximizing the expected significance of $B_s^0 \rightarrow D^+ D_s^-$, $14608 \pm 121 \bar{B}^0$ and $143 \pm 14 B_s^0$ decays are observed (see Fig. 2), from which the ratio extracted is

$$\frac{\mathcal{B}(B_s^0 \rightarrow D^+ D_s^-)}{\mathcal{B}(\bar{B}^0 \rightarrow D^+ D_s^-)} = 0.038 \pm 0.004(\text{stat}) \pm 0.003(\text{syst}).$$

This is the most precise measurement to date of $\mathcal{B}(B_s^0 \rightarrow D^+ D_s^-)$ and supersedes Ref. [36]. Since the two decay modes share the same final state, many systematic uncertainties cancel. The dominant contribution to the uncertainty comes from the beauty-hadron production fractions.

TABLE II. Systematic uncertainties for $M(\Lambda_b^0) - M(\bar{B}^0)$.

Description	Value (MeV/c^2)
$\Lambda_c^+ - D^+$ lifetime difference	0.16
Momentum scale	0.08
Fit model	0.02
Total	0.18

A small additional uncertainty on the efficiency arises due to the uncertainty on the B_s^0 lifetime. Uncertainty in the fit model is largely due to the size of the combinatorial background near the B_s^0 peak. The measured ratio of branching fractions is approximately the ratio of quark-mixing factors, as expected assuming nonfactorizable effects are small.

A search is also performed for the decay modes $B_{(s)}^0 \rightarrow \Lambda_c^+ \Lambda_c^-$. Regions centered around the nominal $B_{(s)}^0$ meson masses with boundaries defined such that each region contains 95% of the corresponding signal are determined using simulation. The expected background contribution in each of these regions is obtained from the charm-hadron mass sidebands. Applying this technique to the $\bar{B}^0 \rightarrow D^+ D_s^-$ and $\Lambda_b^0 \rightarrow \Lambda_c^+ D_{(s)}^-$ decays produces background estimates consistent with those obtained by fitting the invariant mass spectra for those modes. The number of observed candidates in each signal region is then compared to the expected background contribution; no significant excess is observed in either $\Lambda_c^+ \Lambda_c^-$ signal region. The limits obtained using the method of Ref. [37] and the known D_s^- [2], D^- [30], and Λ_c^+ [38] hadron branching fractions are

$$\frac{\mathcal{B}(\bar{B}^0 \rightarrow \Lambda_c^+ \Lambda_c^-)}{\mathcal{B}(\bar{B}^0 \rightarrow D^+ D_s^-)} < 0.0022 [95\% \text{ C.L.}],$$

$$\frac{\mathcal{B}(B_s^0 \rightarrow \Lambda_c^+ \Lambda_c^-)}{\mathcal{B}(B_s^0 \rightarrow D^+ D_s^-)} < 0.30 [95\% \text{ C.L.}].$$

For these results the lifetime of the light-mass B_s^0 eigenstate is assumed, as this produces the most conservative limits [1]. This is the best limit to date for the \bar{B}^0 decay mode and the first limit for the B_s^0 decay mode.

In summary, first observations and relative branching-fraction measurements have been made for the decays $\Lambda_b^0 \rightarrow \Lambda_c^+ D_{(s)}^-$. The most precise measurements of the Λ_b^0 baryon mass and of $\mathcal{B}(B_s^0 \rightarrow D^+ D_s^-)$ have been presented and the most stringent upper limits have been placed on $\mathcal{B}(B_s^0 \rightarrow \Lambda_c^+ \Lambda_c^-)$. Using $\mathcal{B}(\bar{B}^0 \rightarrow D^+ D_s^-) = (7.2 \pm 0.8) \times 10^{-3}$ [2] and $\mathcal{B}(\Lambda_b^0 \rightarrow \Lambda_c^+ \pi^-) / \mathcal{B}(\bar{B}^0 \rightarrow D^+ \pi^-)$ from Ref. [33], the absolute branching fractions obtained are

$$\mathcal{B}(\Lambda_b^0 \rightarrow \Lambda_c^+ D_s^-) = (1.1 \pm 0.1) \times 10^{-2},$$

$$\mathcal{B}(\Lambda_b^0 \rightarrow \Lambda_c^+ D^-) = (4.7 \pm 0.6) \times 10^{-4},$$

$$\mathcal{B}(B_s^0 \rightarrow D^+ D_s^-) = (2.7 \pm 0.5) \times 10^{-4},$$

$$\mathcal{B}(\bar{B}^0 \rightarrow \Lambda_c^+ \Lambda_c^-) < 1.6 \times 10^{-5} [95\% \text{ C.L.}],$$

$$\mathcal{B}(B_s^0 \rightarrow \Lambda_c^+ \Lambda_c^-) < 8.0 \times 10^{-5} [95\% \text{ C.L.}].$$

These results are all consistent with expectations that assume small nonfactorizable effects.

We express our gratitude to our colleagues in the CERN accelerator departments for the excellent performance of the LHC. We thank the technical and administrative staff at the LHCb institutes. We acknowledge support from CERN

and from the national agencies: CAPES, CNPq, FAPERJ, and FINEP (Brazil); NSFC (China); CNRS/IN2P3 and Region Auvergne (France); BMBF, DFG, HGF, and MPG (Germany); SFI (Ireland); INFN (Italy); FOM and NWO (The Netherlands); SCSR (Poland); MEN/IFA (Romania); MinES, Rosatom, RFBR, and NRC ‘‘Kurchatov Institute’’ (Russia); MinECo, XuntaGal, and GENCAT (Spain); SNSF and SER (Switzerland); NAS Ukraine (Ukraine); STFC (United Kingdom); NSF (USA). We also acknowledge the support received from EPLANET and the ERC under FP7. The Tier1 computing centers are supported by IN2P3 (France), KIT and BMBF (Germany), INFN (Italy), NWO and SURF (The Netherlands), PIC (Spain), GridPP (United Kingdom). We are indebted to the communities behind the multiple open-source software packages we depend on. We are also thankful for the computing resources and the access to software R&D tools provided by Yandex LLC (Russia).

-
- [1] Y. Amhis *et al.* (Heavy Flavor Averaging Group), arXiv:1207.1158; updated results and plots available at <http://www.slac.stanford.edu/xorg/hfag/>.
- [2] J. Beringer *et al.* (Particle Data Group), *Phys. Rev. D* **86**, 010001 (2012), and 2013 partial update for the 2014 edition.
- [3] M. Bauer, B. Stech, M. Wirbel, *Z. Phys. C* **34**, 103 (1987).
- [4] C. Amsler, T. Degrand, and B. Krusche, *Quark Model*, in Ref. [2], p. 199.
- [5] M. Karliner, B. Keren-Zur, H. J. Lipkin, and J. L. Rosner, *Ann. Phys. (N.Y.)* **324**, 2 (2009).
- [6] J. P. Day, W. Plessas, and K.-S. Choi, arXiv:1205.6918.
- [7] X. Liu, H.-X. Chen, Y.-R. Liu, A. Hosaka, and S.-L. Zhu, *Phys. Rev. D* **77**, 014031 (2008).
- [8] E. E. Jenkins, *Phys. Rev. D* **77**, 034012 (2008).
- [9] R. Roncaglia, D. Lichtenberg, and E. Predazzi, *Phys. Rev. D* **52**, 1722 (1995).
- [10] N. Mathur, R. Lewis, and R. Woloshyn, *Phys. Rev. D* **66**, 014502 (2002).
- [11] D. Ebert, R. Faustov, and V. Galkin, *Phys. Rev. D* **72**, 034026 (2005).
- [12] R. Aaij *et al.* (LHCb Collaboration), *Phys. Lett. B* **708**, 241 (2012).
- [13] A. A. Alves, Jr. *et al.* (LHCb Collaboration), *JINST* **3**, S08005 (2008).
- [14] R. Arink *et al.*, *JINST* **9**, P01002 (2014).
- [15] M. Adinolfi *et al.*, *Eur. Phys. J. C* **73**, 2431 (2013).
- [16] R. Aaij *et al.*, *JINST* **8**, P04022 (2013).
- [17] A. A. Alves, Jr. *et al.*, *JINST* **8**, P02022 (2013).
- [18] V. V. Gligorov and M. Williams, *JINST* **8**, P02013 (2013).
- [19] T. Sjöstrand, S. Mrenna, and P. Skands, *J. High Energy Phys.* **05** (2006) 026; T. Sjöstrand, S. Mrenna, and P. Skands, *Comput. Phys. Commun.* **178**, 852 (2008).
- [20] I. Belyaev *et al.*, in *Nuclear Science Symposium Conference Record (NSS/MIC)*, Knoxville, 2010 (IEEE, New York, 2010), p. 1155.
- [21] D. J. Lange, *Nucl. Instrum. Methods Phys. Res., Sect. A* **462**, 152 (2001).
- [22] P. Golonka and Z. Was, *Eur. Phys. J. C* **45**, 97 (2006).

- [23] J. Allison *et al.* (GEANT4 Collaboration), *IEEE Trans. Nucl. Sci.* **53**, 270 (2006); S. Agostinelli *et al.* (GEANT4 Collaboration), *Nucl. Instrum. Methods Phys. Res., Sect. A* **506**, 250 (2003).
- [24] M. Clemencic, G. Corti, S. Easo, C. R. Jones, S. Miglioranzi, M. Pappagallo, and P. Robbe, *J. Phys. Conf. Ser.* **331**, 032023 (2011).
- [25] W. D. Hulsbergen, *Nucl. Instrum. Methods Phys. Res., Sect. A* **552**, 566 (2005).
- [26] L. Breiman, J. H. Friedman, R. A. Olshen, and C. J. Stone, *Classification and Regression Trees* (Wadsworth, Belmont, CA, 1984).
- [27] M. Pivk and F. R. Le Diberder, *Nucl. Instrum. Methods Phys. Res., Sect. A* **555**, 356 (2005).
- [28] D. M. Santos and F. Dupertuis, arXiv:1312.5000.
- [29] K. S. Cranmer, *Comput. Phys. Commun.* **136**, 198 (2001).
- [30] G. Bonvicini *et al.* (CLEO Collaboration), *Phys. Rev. D* **89**, 072002 (2014).
- [31] LHCb Collaboration, Report No. LHCb-CONF-2013-011.
- [32] R. Aaij *et al.* (LHCb Collaboration), *Phys. Rev. D* **85**, 032008 (2012).
- [33] R. Aaij *et al.* (LHCb Collaboration), “Measurement of the p_T and η Dependences of Λ_b^0 Production and the $\Lambda_b^0 \rightarrow \Lambda_c^+ \pi^-$ Branching Fraction” (to be published).
- [34] R. Aaij *et al.* (LHCb Collaboration), *J. High Energy Phys.* **06** (2013) 65.
- [35] R. Aaij *et al.* (LHCb Collaboration), *Phys. Rev. Lett.* **110**, 182001 (2013).
- [36] R. Aaij *et al.* (LHCb Collaboration), *Phys. Rev. D* **87**, 092007 (2013).
- [37] W. A. Rolke, A. M. Lopez, and J. Conrad, *Nucl. Instrum. Methods Phys. Res., Sect. A* **551**, 493 (2005).
- [38] A. Zupanc *et al.* (Belle Collaboration), arXiv:1312.7826.

R. Aaij,⁴¹ A. Abba,^{21,a} B. Adeva,³⁷ M. Adinolfi,⁴⁶ A. Affolder,⁵² Z. Ajaltouni,⁵ J. Albrecht,⁹ F. Alessio,³⁸ M. Alexander,⁵¹ S. Ali,⁴¹ G. Alkhazov,³⁰ P. Alvarez Cartelle,³⁷ A. A. Alves Jr.,^{25,38} S. Amato,² S. Amerio,²² Y. Amhis,⁷ L. An,³ L. Anderlini,^{17,b} J. Anderson,⁴⁰ R. Andreassen,⁵⁷ M. Andreotti,^{16,c} J. E. Andrews,⁵⁸ R. B. Appleby,⁵⁴ O. Aquines Gutierrez,¹⁰ F. Archilli,³⁸ A. Artamonov,³⁵ M. Artuso,⁵⁹ E. Aslanides,⁶ G. Auriemma,^{25,d} M. Baalouch,⁵ S. Bachmann,¹¹ J. J. Back,⁴⁸ A. Badalov,³⁶ V. Balagura,³¹ W. Baldini,¹⁶ R. J. Barlow,⁵⁴ C. Barschel,³⁸ S. Barsuk,⁷ W. Barter,⁴⁷ V. Batozskaya,²⁸ T. Bauer,⁴¹ A. Bay,³⁹ J. Beddow,⁵¹ F. Bedeschi,²³ I. Bediaga,¹ S. Belogurov,³¹ K. Belous,³⁵ I. Belyaev,³¹ E. Ben-Haim,⁸ G. Bencivenni,¹⁸ S. Benson,⁵⁰ J. Benton,⁴⁶ A. Bereznoi,³² R. Bernet,⁴⁰ M.-O. Bettler,⁴⁷ M. van Beuzekom,⁴¹ A. Bien,¹¹ S. Bifani,⁴⁵ T. Bird,⁵⁴ A. Bizzeti,^{17,e} P. M. Björnstad,⁵⁴ T. Blake,⁴⁸ F. Blanc,³⁹ J. Blouw,¹⁰ S. Blusk,⁵⁹ V. Bocci,²⁵ A. Bondar,³⁴ N. Bondar,^{30,38} W. Bonivento,^{15,38} S. Borghi,⁵⁴ A. Borgia,⁵⁹ M. Borsato,⁷ T. J. V. Bowcock,⁵² E. Bowen,⁴⁰ C. Bozzi,¹⁶ T. Brambach,⁹ J. van den Brand,⁴² J. Bressieux,³⁹ D. Brett,⁵⁴ M. Britsch,¹⁰ T. Britton,⁵⁹ N. H. Brook,⁴⁶ H. Brown,⁵² A. Bursche,⁴⁰ G. Busetto,^{22,f} J. Buytaert,³⁸ S. Cadeddu,¹⁵ R. Calabrese,^{16,c} O. Callot,⁷ M. Calvi,^{20,g} M. Calvo Gomez,^{36,h} A. Camboni,³⁶ P. Campana,^{18,38} D. Campora Perez,³⁸ F. Caponio,^{21,a} A. Carbone,^{14,i} G. Carboni,^{24,j} R. Cardinale,^{19,38,k} A. Cardini,¹⁵ H. Carranza-Mejia,⁵⁰ L. Carson,⁵⁰ K. Carvalho Akiba,² G. Casse,⁵² L. Cassina,²⁰ L. Castillo Garcia,³⁸ M. Cattaneo,³⁸ C. Cauet,⁹ R. Cenci,⁵⁸ M. Charles,⁸ P. Charpentier,³⁸ S.-F. Cheung,⁵⁵ N. Chiapolini,⁴⁰ M. Chrzascz,^{40,26} K. Ciba,³⁸ X. Cid Vidal,³⁸ G. Ciezarek,⁵³ P. E. L. Clarke,⁵⁰ M. Clemencic,³⁸ H. V. Cliff,⁴⁷ J. Closier,³⁸ C. Coca,²⁹ V. Coco,³⁸ J. Cogan,⁶ E. Cogneras,⁵ P. Collins,³⁸ A. Comerma-Montells,³⁶ A. Contu,^{15,38} A. Cook,⁴⁶ M. Coombes,⁴⁶ S. Coquereau,⁸ G. Corti,³⁸ M. Corvo,^{16,c} I. Counts,⁵⁶ B. Couturier,³⁸ G. A. Cowan,⁵⁰ D. C. Craik,⁴⁸ M. Cruz Torres,⁶⁰ A. R. Cukierman,⁵⁶ S. Cunliffe,⁵³ R. Currie,⁵⁰ C. D’Ambrosio,³⁸ J. Dalseno,⁴⁶ P. David,⁸ P. N. Y. David,⁴¹ A. Davis,⁵⁷ K. De Bruyn,⁴¹ S. De Capua,⁵⁴ M. De Cian,¹¹ J. M. De Miranda,¹ L. De Paula,² W. De Silva,⁵⁷ P. De Simone,¹⁸ D. Decamp,⁴ M. Deckenhoff,⁹ L. Del Buono,⁸ N. Déleage,⁴ D. Derkach,⁵⁵ O. Deschamps,⁵ F. Dettori,⁴² A. Di Canto,³⁸ H. Dijkstra,³⁸ S. Donleavy,⁵² F. Dordei,¹¹ M. Dorigo,³⁹ C. Dorothy,⁵⁶ A. Dosil Suárez,³⁷ D. Dossett,⁴⁸ A. Dovbnya,⁴³ F. Dupertuis,³⁹ P. Durante,³⁸ R. Dzhelyadin,³⁵ A. Dziurda,²⁶ A. Dzyuba,³⁰ S. Easo,⁴⁹ U. Egede,⁵³ V. Egorychev,³¹ S. Eidelman,³⁴ S. Eisenhardt,⁵⁰ U. Eitschberger,⁹ R. Ekelhof,⁹ L. Eklund,^{51,38} I. El Rifai,⁵ C. Elsasser,⁴⁰ S. Esen,¹¹ T. Evans,⁵⁵ A. Falabella,^{16,c} C. Färber,¹¹ C. Farinelli,⁴¹ S. Farry,⁵² D. Ferguson,⁵⁰ V. Fernandez Albor,³⁷ F. Ferreira Rodrigues,¹ M. Ferro-Luzzi,³⁸ S. Filippov,³³ M. Fiore,^{16,c} M. Fiorini,^{16,c} M. Firlej,²⁷ C. Fitzpatrick,³⁸ T. Fiutowski,²⁷ M. Fontana,¹⁰ F. Fontanelli,^{19,k} R. Forty,³⁸ O. Francisco,² M. Frank,³⁸ C. Frei,³⁸ M. Frosini,^{17,38,b} J. Fu,²¹ E. Furfaro,^{24,j} A. Gallas Torreira,³⁷ D. Galli,^{14,i} S. Gambetta,^{19,k} M. Gandelman,² P. Gandini,⁵⁹ Y. Gao,³ J. Garofoli,⁵⁹ J. Garra Tico,⁴⁷ L. Garrido,³⁶ C. Gaspar,³⁸ R. Gauld,⁵⁵ L. Gavardi,⁹ E. Gersabeck,¹¹ M. Gersabeck,⁵⁴ T. Gershon,⁴⁸ P. Ghez,⁴ A. Gianelle,²² S. Giani,³⁹ V. Gibson,⁴⁷ L. Giubega,²⁹ V. V. Gligorov,³⁸ C. Göbel,⁶⁰ D. Golubkov,³¹ A. Golutvin,^{53,31,38} A. Gomes,^{1,1} H. Gordon,³⁸ C. Gotti,²⁰ M. Grabalosa Gándara,⁵ R. Graciani Diaz,³⁶ L. A. Granado Cardoso,³⁸ E. Graugés,³⁶ G. Graziani,¹⁷ A. Grecu,²⁹ E. Greening,⁵⁵ S. Gregson,⁴⁷ P. Griffith,⁴⁵ L. Grillo,¹¹ O. Grünberg,⁶² B. Gui,⁵⁹ E. Gushchin,³³ Y. Guz,^{35,38} T. Gys,³⁸ C. Hadjivasiliou,⁵⁹ G. Haefeli,³⁹ C. Haen,³⁸ S. C. Haines,⁴⁷ S. Hall,⁵³ B. Hamilton,⁵⁸ T. Hampson,⁴⁶ X. Han,¹¹

S. Hansmann-Menzemer,¹¹ N. Harnew,⁵⁵ S. T. Harnew,⁴⁶ J. Harrison,⁵⁴ T. Hartmann,⁶² J. He,³⁸ T. Head,³⁸ V. Heijne,⁴¹ K. Hennessy,⁵² P. Henrard,⁵ L. Henry,⁸ J. A. Hernando Morata,³⁷ E. van Herwijnen,³⁸ M. Heß,⁶² A. Hicheur,¹ D. Hill,⁵⁵ M. Hoballah,⁵ C. Hombach,⁵⁴ W. Hulsbergen,⁴¹ P. Hunt,⁵⁵ N. Hussain,⁵⁵ D. Hutchcroft,⁵² D. Hynds,⁵¹ M. Idzik,²⁷ P. Ilten,⁵⁶ R. Jacobsson,³⁸ A. Jaeger,¹¹ J. Jalocha,⁵⁵ E. Jans,⁴¹ P. Jaton,³⁹ A. Jawahery,⁵⁸ M. Jezabek,²⁶ F. Jing,³ M. John,⁵⁵ D. Johnson,⁵⁵ C. R. Jones,⁴⁷ C. Joram,³⁸ B. Jost,³⁸ N. Jurik,⁵⁹ M. Kabbalo,⁹ S. Kandybei,⁴³ W. Kanso,⁶ M. Karacson,³⁸ T. M. Karbach,³⁸ M. Kelsey,⁵⁹ I. R. Kenyon,⁴⁵ T. Ketel,⁴² B. Khanji,²⁰ C. Khurewathanakul,³⁹ S. Klaver,⁵⁴ O. Kochebina,⁷ M. Kolpin,¹¹ I. Komarov,³⁹ R. F. Koopman,⁴² P. Koppenburg,^{41,38} M. Korolev,³² A. Kozlinskiy,⁴¹ L. Kravchuk,³³ K. Kreplin,¹¹ M. Krepis,⁴⁸ G. Krocker,¹¹ P. Krokovny,³⁴ F. Kruse,⁹ M. Kucharczyk,^{20,26,38,g} V. Kudryavtsev,³⁴ K. Kurek,²⁸ T. Kvaratskheliya,³¹ V. N. La Thi,³⁹ D. Lacarrere,³⁸ G. Lafferty,⁵⁴ A. Lai,¹⁵ D. Lambert,⁵⁰ R. W. Lambert,⁴² E. Lanciotti,³⁸ G. Lanfranchi,¹⁸ C. Langenbruch,³⁸ B. Langhans,³⁸ T. Latham,⁴⁸ C. Lazzeroni,⁴⁵ R. Le Gac,⁶ J. van Leerdam,⁴¹ J.-P. Lees,⁴ R. Lefèvre,⁵ A. Leflat,³² J. Lefrançois,⁷ S. Leo,²³ O. Leroy,⁶ T. Lesiak,²⁶ B. Leverington,¹¹ Y. Li,³ M. Liles,⁵² R. Lindner,³⁸ C. Linn,³⁸ F. Lionetto,⁴⁰ B. Liu,¹⁵ G. Liu,³⁸ S. Lohn,³⁸ I. Longstaff,⁵¹ I. Longstaff,⁵¹ J. H. Lopes,² N. Lopez-March,³⁹ P. Lowdon,⁴⁰ H. Lu,³ D. Lucchesi,^{22,f} H. Luo,⁵⁰ A. Lupato,²² E. Luppi,^{16,c} O. Lupton,⁵⁵ F. Machefert,⁷ I. V. Machikhiliyan,³¹ F. Maciuc,²⁹ O. Maev,³⁰ S. Malde,⁵⁵ G. Manca,^{15,m} G. Mancinelli,⁶ M. Manzali,^{16,c} J. Maratas,⁵ J. F. Marchand,⁴ U. Marconi,¹⁴ C. Marin Benito,³⁶ P. Marino,^{23,n} R. Märki,³⁹ J. Marks,¹¹ G. Martellotti,²⁵ A. Martens,⁸ A. Martín Sánchez,⁷ M. Martinelli,⁴¹ D. Martinez Santos,⁴² F. Martinez Vidal,⁶⁴ D. Martins Tostes,² A. Massafferri,¹ R. Matev,³⁸ Z. Mathe,³⁸ C. Matteuzzi,²⁰ A. Mazurov,^{16,38,c} M. McCann,⁵³ J. McCarthy,⁴⁵ A. McNab,⁵⁴ R. McNulty,¹² B. McSkelly,⁵² B. Meadows,^{57,55} F. Meier,⁹ M. Meissner,¹¹ M. Merk,⁴¹ D. A. Milanese,⁸ M.-N. Minard,⁴ J. Molina Rodriguez,⁶⁰ S. Monteil,⁵ D. Moran,⁵⁴ M. Morandin,²² P. Morawski,²⁶ A. Mordà,⁶ M. J. Morello,^{23,n} J. Moron,²⁷ R. Mountain,⁵⁹ F. Muheim,⁵⁰ K. Müller,⁴⁰ R. Muresan,²⁹ B. Muster,³⁹ P. Naik,⁴⁶ T. Nakada,³⁹ R. Nandakumar,⁴⁹ I. Nasteva,¹ M. Needham,⁵⁰ N. Neri,²¹ S. Neubert,³⁸ N. Neufeld,³⁸ M. Neuner,¹¹ A. D. Nguyen,³⁹ T. D. Nguyen,³⁹ C. Nguyen-Mau,^{39,o} M. Nicol,⁷ V. Niess,⁵ R. Niet,⁹ N. Nikitin,³² T. Nikodem,¹¹ A. Novoselov,³⁵ A. Oblakowska-Mucha,²⁷ V. Obraztsov,³⁵ S. Oggero,⁴¹ S. Ogilvy,⁵¹ O. Okhrimenko,⁴⁴ R. Oldeman,^{15,m} G. Onderwater,⁶⁵ M. Orlandea,²⁹ J. M. Otalora Goicochea,² P. Owen,⁵³ A. Oyanguren,⁶⁴ B. K. Pal,⁵⁹ A. Palano,^{13,p} F. Palombo,^{21,q} M. Palutan,¹⁸ J. Panman,³⁸ A. Papanestis,^{49,38} M. Pappagallo,⁵¹ C. Parkes,⁵⁴ C. J. Parkinson,⁹ G. Passaleva,¹⁷ G. D. Patel,⁵² M. Patel,⁵³ C. Patrignani,^{19,k} A. Pazos Alvarez,³⁷ A. Pearce,⁵⁴ A. Pellegrino,⁴¹ M. Pepe Altarelli,³⁸ S. Perazzini,^{14,i} E. Perez Trigo,³⁷ P. Perret,⁵ M. Perrin-Terrin,⁶ L. Pescatore,⁴⁵ E. Pesen,⁶⁶ K. Petridis,⁵³ A. Petrolini,^{19,k} E. Picatoste Olloqui,³⁶ B. Pietrzyk,⁴ T. Pilař,⁴⁸ D. Pinci,²⁵ A. Pistone,¹⁹ S. Playfer,⁵⁰ M. Plo Casasus,³⁷ F. Polci,⁸ A. Poluektov,^{48,34} E. Polycarpo,² A. Popov,³⁵ D. Popov,¹⁰ B. Popovici,²⁹ C. Potterat,² A. Powell,⁵⁵ J. Prisciandaro,³⁹ A. Pritchard,⁵² C. Prouve,⁴⁶ V. Pugatch,⁴⁴ A. Puig Navarro,³⁹ G. Punzi,^{23,r} W. Qian,⁴ B. Rachwal,²⁶ J. H. Rademacker,⁴⁶ B. Rakotomiramanana,³⁹ M. Rama,¹⁸ M. S. Rangel,² I. Raniuk,⁴³ N. Rauschmayr,³⁸ G. Raven,⁴² S. Reichert,⁵⁴ M. M. Reid,⁴⁸ A. C. dos Reis,¹ S. Ricciardi,⁴⁹ A. Richards,⁵³ K. Rinnert,⁵² V. Rives Molina,³⁶ D. A. Roa Romero,⁵ P. Robbe,⁷ A. B. Rodrigues,¹ E. Rodrigues,⁵⁴ P. Rodriguez Perez,⁵⁴ S. Roiser,³⁸ V. Romanovsky,³⁵ A. Romero Vidal,³⁷ M. Rotondo,²² J. Rouvinet,³⁹ T. Ruf,³⁸ F. Ruffini,²³ H. Ruiz,³⁶ P. Ruiz Valls,⁶⁴ G. Sabatino,^{25,j} J. J. Saborido Silva,³⁷ N. Sagidova,³⁰ P. Sail,⁵¹ B. Saitta,^{15,m} V. Salustino Guimaraes,² C. Sanchez Mayordomo,⁶⁴ B. Sanmartin Sedes,³⁷ R. Santacesaria,²⁵ C. Santamarina Rios,³⁷ E. Santovetti,^{24,j} M. Sapunov,⁶ A. Sarti,^{18,s} C. Satriano,^{25,d} A. Satta,²⁴ M. Savrie,¹⁶ D. Savrina,^{31,32} M. Schiller,⁴² H. Schindler,³⁸ M. Schlupp,⁹ M. Schmelling,¹⁰ B. Schmidt,³⁸ O. Schneider,³⁹ A. Schopper,³⁸ M.-H. Schune,⁷ R. Schwemmer,³⁸ B. Sciascia,¹⁸ A. Sciubba,²⁵ M. Seco,³⁷ A. Semennikov,³¹ K. Senderowska,²⁷ I. Sepp,⁵³ N. Serra,⁴⁰ J. Serrano,⁶ L. Sestini,²² P. Seyfert,¹¹ M. Shapkin,³⁵ I. Shapoval,^{16,43,c} Y. Shcheglov,³⁰ T. Shears,⁵² L. Shekhtman,³⁴ V. Shevchenko,⁶³ A. Shires,⁹ R. Silva Coutinho,⁴⁸ G. Simi,²² M. Sirendi,⁴⁷ N. Skidmore,⁴⁶ T. Skwarnicki,⁵⁹ N. A. Smith,⁵² E. Smith,^{55,49} E. Smith,⁵³ J. Smith,⁴⁷ M. Smith,⁵⁴ H. Snoek,⁴¹ M. D. Sokoloff,⁵⁷ F. J. P. Soler,⁵¹ F. Soomro,³⁹ D. Souza,⁴⁶ B. Souza De Paula,² B. Spaan,⁹ A. Sparkes,⁵⁰ F. Spinella,²³ P. Spradlin,⁵¹ F. Stagni,³⁸ S. Stahl,¹¹ O. Steinkamp,⁴⁰ O. Stenyakin,³⁵ S. Stevenson,⁵⁵ S. Stoica,²⁹ S. Stone,⁵⁹ B. Storaci,⁴⁰ S. Stracka,^{23,38} M. Straticiu,²⁹ U. Straumann,⁴⁰ R. Stroili,²² V. K. Subbiah,³⁸ L. Sun,⁵⁷ W. Sutcliffe,⁵³ K. Swientek,²⁷ S. Swientek,⁹ V. Syropoulos,⁴² M. Szczekowski,²⁸ P. Szczypka,^{39,38} D. Szilard,² T. Szumlak,²⁷ S. T. Jampens,⁴ M. Teklishyn,⁷ G. Tellarini,^{16,c} E. Teodorescu,²⁹ F. Teubert,³⁸ C. Thomas,⁵⁵ E. Thomas,³⁸ J. van Tilburg,⁴¹ V. Tisserand,⁴ M. Tobin,³⁹ S. Tolk,⁴² L. Tomassetti,^{16,c} D. Tonelli,³⁸ S. Topp-Joergensen,⁵⁵ N. Torr,⁵⁵ E. Tournefier,⁴ S. Tourneur,³⁹ M. T. Tran,³⁹ M. Tresch,⁴⁰ A. Tsaregorodtsev,⁶ P. Tsopelas,⁴¹ N. Tuning,⁴¹ M. Ubeda Garcia,³⁸ A. Ukleja,²⁸ A. Ustyuzhanin,⁶³ U. Uwer,¹¹ V. Vagnoni,¹⁴ G. Valenti,¹⁴ A. Vallier,⁷ R. Vazquez Gomez,¹⁸ P. Vazquez Regueiro,³⁷ C. Vázquez Sierra,³⁷ S. Vecchi,¹⁶ J. J. Velthuis,⁴⁶ M. Veltri,^{17,i} G. Veneziano,³⁹ M. Vesterinen,¹¹ B. Viaud,⁷ D. Vieira,² M. Vieites Diaz,³⁷ X. Vilasis-Cardona,^{36,h} A. Vollhardt,⁴⁰ D. Volyansky,¹⁰

D. Voong,⁴⁶ A. Vorobyev,³⁰ V. Vorobyev,³⁴ C. Voß,⁶² H. Voss,¹⁰ J. A. de Vries,⁴¹ R. Waldi,⁶² C. Wallace,⁴⁸ R. Wallace,¹² J. Walsh,²³ S. Wandernoth,¹¹ J. Wang,⁵⁹ D. R. Ward,⁴⁷ N. K. Watson,⁴⁵ A. D. Webber,⁵⁴ D. Websdale,⁵³ M. Whitehead,⁴⁸ J. Wicht,³⁸ D. Wiedner,¹¹ G. Wilkinson,⁵⁵ M. P. Williams,⁴⁵ M. Williams,⁵⁶ F. F. Wilson,⁴⁹ J. Wimberley,⁵⁸ J. Wishahi,⁹ W. Wislicki,²⁸ M. Witek,²⁶ G. Wormser,⁷ S. A. Wotton,⁴⁷ S. Wright,⁴⁷ S. Wu,³ K. Wyllie,³⁸ Y. Xie,⁶¹ Z. Xing,⁵⁹ Z. Xu,³⁹ Z. Yang,³ X. Yuan,³ O. Yushchenko,³⁵ M. Zangoli,¹⁴ M. Zavertyaev,^{10,u} F. Zhang,³ L. Zhang,⁵⁹ W. C. Zhang,¹² Y. Zhang,³ A. Zhelezov,¹¹ A. Zhokhov,³¹ L. Zhong,³ and A. Zvyagin³⁸

(LHCb Collaboration)

- ¹Centro Brasileiro de Pesquisas Físicas (CBPF), Rio de Janeiro, Brazil
²Universidade Federal do Rio de Janeiro (UFRJ), Rio de Janeiro, Brazil
³Center for High Energy Physics, Tsinghua University, Beijing, China
⁴LAPP, Université de Savoie, CNRS/IN2P3, Annecy-Le-Vieux, France
⁵Clermont Université, Université Blaise Pascal, CNRS/IN2P3, LPC, Clermont-Ferrand, France
⁶CPPM, Aix-Marseille Université, CNRS/IN2P3, Marseille, France
⁷LAL, Université Paris-Sud, CNRS/IN2P3, Orsay, France
⁸LPNHE, Université Pierre et Marie Curie, Université Paris Diderot, CNRS/IN2P3, Paris, France
⁹Fakultät Physik, Technische Universität Dortmund, Dortmund, Germany
¹⁰Max-Planck-Institut für Kernphysik (MPIK), Heidelberg, Germany
¹¹Physikalisches Institut, Ruprecht-Karls-Universität Heidelberg, Heidelberg, Germany
¹²School of Physics, University College Dublin, Dublin, Ireland
¹³Sezione INFN di Bari, Bari, Italy
¹⁴Sezione INFN di Bologna, Bologna, Italy
¹⁵Sezione INFN di Cagliari, Cagliari, Italy
¹⁶Sezione INFN di Ferrara, Ferrara, Italy
¹⁷Sezione INFN di Firenze, Firenze, Italy
¹⁸Laboratori Nazionali dell'INFN di Frascati, Frascati, Italy
¹⁹Sezione INFN di Genova, Genova, Italy
²⁰Sezione INFN di Milano Bicocca, Milano, Italy
²¹Sezione INFN di Milano, Milano, Italy
²²Sezione INFN di Padova, Padova, Italy
²³Sezione INFN di Pisa, Pisa, Italy
²⁴Sezione INFN di Roma Tor Vergata, Roma, Italy
²⁵Sezione INFN di Roma La Sapienza, Roma, Italy
²⁶Henryk Niewodniczanski Institute of Nuclear Physics Polish Academy of Sciences, Kraków, Poland
²⁷AGH - University of Science and Technology, Faculty of Physics and Applied Computer Science, Kraków, Poland
²⁸National Center for Nuclear Research (NCBJ), Warsaw, Poland
²⁹Horia Hulubei National Institute of Physics and Nuclear Engineering, Bucharest-Magurele, Romania
³⁰Petersburg Nuclear Physics Institute (PNPI), Gatchina, Russia
³¹Institute of Theoretical and Experimental Physics (ITEP), Moscow, Russia
³²Institute of Nuclear Physics, Moscow State University (SINP MSU), Moscow, Russia
³³Institute for Nuclear Research of the Russian Academy of Sciences (INR RAN), Moscow, Russia
³⁴Budker Institute of Nuclear Physics (SB RAS) and Novosibirsk State University, Novosibirsk, Russia
³⁵Institute for High Energy Physics (IHEP), Protvino, Russia
³⁶Universitat de Barcelona, Barcelona, Spain
³⁷Universidad de Santiago de Compostela, Santiago de Compostela, Spain
³⁸European Organization for Nuclear Research (CERN), Geneva, Switzerland
³⁹Ecole Polytechnique Fédérale de Lausanne (EPFL), Lausanne, Switzerland
⁴⁰Physik-Institut, Universität Zürich, Zürich, Switzerland
⁴¹Nikhef National Institute for Subatomic Physics, Amsterdam, The Netherlands
⁴²Nikhef National Institute for Subatomic Physics and VU University Amsterdam, Amsterdam, The Netherlands
⁴³NSC Kharkiv Institute of Physics and Technology (NSC KIPT), Kharkiv, Ukraine
⁴⁴Institute for Nuclear Research of the National Academy of Sciences (KINR), Kyiv, Ukraine
⁴⁵University of Birmingham, Birmingham, United Kingdom
⁴⁶H.H. Wills Physics Laboratory, University of Bristol, Bristol, United Kingdom
⁴⁷Cavendish Laboratory, University of Cambridge, Cambridge, United Kingdom
⁴⁸Department of Physics, University of Warwick, Coventry, United Kingdom
⁴⁹STFC Rutherford Appleton Laboratory, Didcot, United Kingdom

- ⁵⁰*School of Physics and Astronomy, University of Edinburgh, Edinburgh, United Kingdom*
⁵¹*School of Physics and Astronomy, University of Glasgow, Glasgow, United Kingdom*
⁵²*Oliver Lodge Laboratory, University of Liverpool, Liverpool, United Kingdom*
⁵³*Imperial College London, London, United Kingdom*
⁵⁴*School of Physics and Astronomy, University of Manchester, Manchester, United Kingdom*
⁵⁵*Department of Physics, University of Oxford, Oxford, United Kingdom*
⁵⁶*Massachusetts Institute of Technology, Cambridge, Massachusetts, USA*
⁵⁷*University of Cincinnati, Cincinnati, Ohio, USA*
⁵⁸*University of Maryland, College Park, Maryland, USA*
⁵⁹*Syracuse University, Syracuse, New York, USA*
⁶⁰*Pontifícia Universidade Católica do Rio de Janeiro (PUC-Rio), Rio de Janeiro, Brazil (associated with Universidade Federal do Rio de Janeiro (UFRJ), Rio de Janeiro, Brazil)*
⁶¹*Institute of Particle Physics, Central China Normal University, Wuhan, Hubei, China (associated with Center for High Energy Physics, Tsinghua University, Beijing, China)*
⁶²*Institut für Physik, Universität Rostock, Rostock, Germany (associated with Physikalisches Institut, Ruprecht-Karls-Universität Heidelberg, Heidelberg, Germany)*
⁶³*National Research Centre Kurchatov Institute, Moscow, Russia (associated with Institute of Theoretical and Experimental Physics [ITEP], Moscow, Russia)*
⁶⁴*Instituto de Física Corpuscular (IFIC), Universitat de Valencia-CSIC, Valencia, Spain (associated with Universitat de Barcelona, Barcelona, Spain)*
⁶⁵*KVI-University of Groningen, Groningen, The Netherlands (associated with Nikhef National Institute for Subatomic Physics, Amsterdam, The Netherlands)*
⁶⁶*Celal Bayar University, Manisa, Turkey (associated with European Organization for Nuclear Research [CERN], Geneva, Switzerland)*

^aAlso at Politecnico di Milano, Milano, Italy.

^bAlso at Università di Firenze, Firenze, Italy.

^cAlso at Università di Ferrara, Ferrara, Italy.

^dAlso at Università della Basilicata, Potenza, Italy.

^eAlso at Università di Modena e Reggio Emilia, Modena, Italy.

^fAlso at Università di Padova, Padova, Italy.

^gAlso at Università di Milano Bicocca, Milano, Italy.

^hAlso at LIFAELS, La Salle, Universitat Ramon Llull, Barcelona, Spain.

ⁱAlso at Università di Bologna, Bologna, Italy.

^jAlso at Università di Roma Tor Vergata, Roma, Italy.

^kAlso at Università di Genova, Genova, Italy.

^lAlso at Universidade Federal do Triângulo Mineiro (UFTM), Uberaba-MG, Brazil.

^mAlso at Università di Cagliari, Cagliari, Italy.

ⁿAlso at Scuola Normale Superiore, Pisa, Italy.

^oAlso at Hanoi University of Science, Hanoi, Viet Nam.

^pAlso at Università di Bari, Bari, Italy.

^qAlso at Università degli Studi di Milano, Milano, Italy.

^rAlso at Università di Pisa, Pisa, Italy.

^sAlso at Università di Roma La Sapienza, Roma, Italy.

^tAlso at Università di Urbino, Urbino, Italy.

^uAlso at P.N. Lebedev Physical Institute, Russian Academy of Science (LPI RAS), Moscow, Russia.